University Turbine Systems Research (UTSR)
2016 Gas Turbine Industrial Fellowship Program

Modification of Heat Release Model in General Instability Model (GIM) for Optimization of Burner Configuration for Instability Mitigation

Prepared for

Siemens Energy
Orlando, FL 32826

and

Southwest Research Institute
San Antonio, TX 78228

Prepared by

Daniel Depperschmidt
The University of Alabama
Department of Mechanical Engineering
Tuscaloosa, AL 35401

Abstract

Siemens has been actively co-developing a tool known as the generalized instability model (GIM) to provide low order analytical models to investigate the relationships between combustion processes and transverse acoustic modes within the combustion chamber. This tool is to be used to analyze the heat release/pressure mode relationship prior to conducting experimentation.

GIM is to be used as a computationally inexpensive analysis technique to conduct such a study. However, until now the GIM tool was unable to generate unique heat release profiles due to the inability modify the combustor configuration on a per element basis.

The goal of this study is to extend the ability of GIM to model unique burner configurations and to then correlate relationships between combustor geometry and instability growth rate by allowing the user to specify the position, fuel staging and flame front of each individual burner element.

Introduction/Background

It is widely accepted that lean premixed combustion implemented in stationary gas turbines is an efficient means of energy production, capable of achieving high power output while minimizing the production of harmful emissions. However, a significant drawback to the lean premixed combustion process is the inherent susceptibility to the development and propagation of thermoacoustic instabilities. These instabilities result in strong pressure oscillations which can potentially cause permanent damage to gas turbine engine components. It is therefore paramount to develop strategies to mitigate the development of these instabilities.

There are multiple approaches to reduce the propagation of instabilities or the subsequent pressure oscillations that accompany their development. These approaches can be subcategorized into active and passive mitigation techniques. Active mitigation can be adapted to many different operational and geometric conditions and entails altering the operating conditions to conduct combustion less susceptible to the development of instabilities [1]. Passive mitigation often utilizes a geometric alteration of the combustor or its components to prevent instabilities or to dampen the pressure oscillations which are generated [2]. Figure 1 illustrates the advantages of an active mitigation technique.

From this sketch, it can be seen that the growth of instability follows a logarithmic curve which tends to plateau at elevated net acoustical energy outputs, while the losses of the same instability follow a linear curve. The circle symbol represents the cyclical saturation point, or limit cycle amplitude. From this condition, the pressure oscillations must be reduced. If an active mitigation technique is chosen in which the driving of the instabilities is reduced (represented by arrow A), the limit cycle amplitude limit will be reached at the square symbol. If a passive mitigation technique is employed which reduces the amount of net acoustic energy added to the system (represented by arrow B), the cyclic amplitude limit is reached at the triangle symbol.

One proposed method of limiting the excitation of instabilities is to configure the elements of the combustor in an asymmetric pattern to limit the energy which is generated within the regions of the domain at the antinodes of a transverse mode. In order to investigate the efficacy of such a technique using a low order modeling tool such as GIM, the heat release model must be modified to permit the user to specify the exact position and alter the relative fuel staging of each individual heating element. This report describes the manner in which the mean heat release model of GIM was modified to allow for such an investigation, and the results of the subsequent

study to inspect the trends that may develop regarding the relationship between the geometry of a heat release profile and the growth rate of HFD.

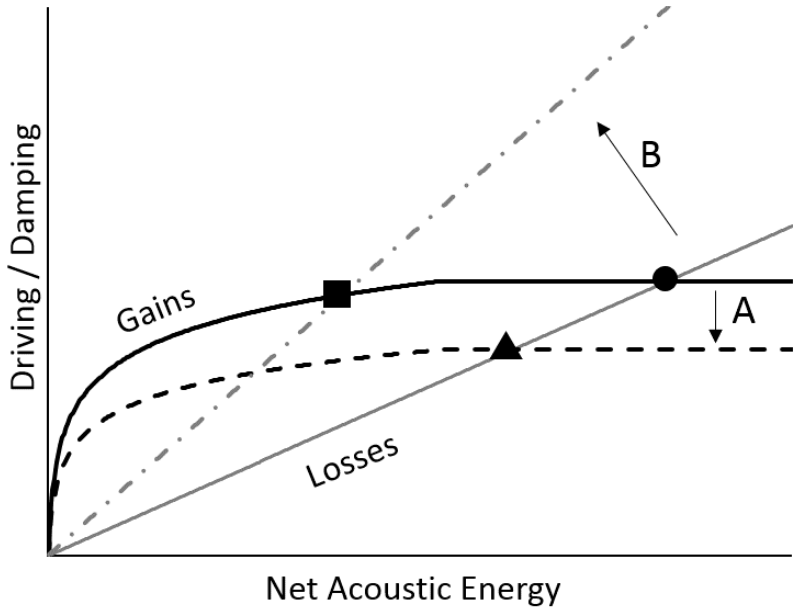

Figure 1. Driving/damping comparison.

GIM Governing Equations

This section will detail some of the governing equations used in GIM to characterize pressure and velocity fluctuations will now be detailed and follows the method described by Pent et al [3]. GIM solves an unsteady, inhomogeneous wave equation for the acoustic pressure perturbation, *p'*, of the gas phase inside a combustion chamber as

$$\nabla^2 p' - \frac{1}{c^2}\frac{\partial^2 p'}{\partial t^2} = h \tag{1}$$

with wall boundary conditions

$$\hat{n} \cdot \nabla p' = -f \tag{2}$$

where

c is the sonic velocity,

$\hat{n}$ is the unit normal vector,

and *h* and *f* are inhomogeneous terms used to include other effects including unsteady combustion processes, damping mechanisms, mean flow variations, and nonlinear effects such as higher order acoustics, mean flow, and acoustic interactions.

The perturbation variables are then split into temporal and spatial modes via a modified Galerkin method as a solution to equation 1, based off the developments by Culik et al. [4]. The pressure and velocity perturbation variables are defined as follows

$$p'(x,r,\theta,t) = \bar{p}\sum_{n=1}^{N}\psi_n(x)\psi_n(r,\theta)\eta_n(t) \tag{3}$$

$$u'(x,r,\theta,t) = \sum_{n=1}^{N}\frac{1}{\gamma k_n^2}\nabla\psi_n(x)\nabla\psi_n(r,\theta)\dot{\eta}_n(t) \tag{4}$$

where the velocity perturbation equation is derived from the continuity equation.

Here it can be seen that the Galerkin method effectively decouples the wave equation into two ordinary differential equations. This is done by applying trial functions ψ_n which is only dependent upon the spatial coordinate, and η_n, which is dependent only upon time. ψ_n is then further reduced to two functions with $\psi_n(x)$ and $\psi_n(r, \Theta)$. Breaking this trial function into these components results in a quasi-3D formulation and enables fast solutions to 3D models with small penalties in accuracy when applied on simple models.

The trial functions are then set to be equal to the eigenmodes of the system which allows for the total solution to be described as the sum over all modes, shown as

$$\nabla^2\psi_n + k_n^2\psi_n = 0 \tag{5}$$

Using this relationship, a set of second order inhomogeneous differential equations are established which relates the temporal trial functions and wave number to a forcing term which represents the inhomogeneous portion of the wave equation as

$$\ddot{\eta}_n + \omega_n^2\eta_n = F_n \tag{6}$$

This portion also includes terms characterizing the boundary conditions of the system and the forcing due to unsteadiness of the combustion process. When deriving the governing equations for GIM, it is assumed that the acoustic fluctuations are linear, which is a valid assumption when the acoustic pressures are relatively small compared to the mean pressure. For more detailed derivations of the equations used by GIM, refer to Portillo, et al 2007 [5].

For the purposes of this study, the only variance from previous GIM models resides in the distribution of the mean heat release profile. The function generates a 2D domain to represent the distribution of energy released during the combustion process as heat. This distribution is normalized such that the integral of entire domain is equal to 1. Thus, the energy contributed to the growth or decay of the instability is independent of the quantity of elements in the burner configuration. The heat release profile is then integrated in the z-direction, resulting in a quasi-3D mean heat release model. This mean heat release value is then used to calculate the unsteady heat release, which is integrated across the volume when calculating the source term for the forcing function used in growth rate evaluation. The fluctuations of heat release relative to the mean heat release are based off of NASA's SP194 document on Liquid Propellant Rocket Combustion Instability [6] and are defined as

$$\frac{q'}{\overline{Q}}(r,\theta,z,t)=\frac{n}{\overline{p}}\delta_{r,\theta}\delta_z p'(r,\theta)p'(z_o,t-\tau) \tag{7}$$

The unsteady heat release rate is then defined as

$$\frac{\partial q'}{\partial t}=n\overline{Q}\,\psi\dot{\eta} \tag{8}$$

which contributes to the previously described forcing function when evaluating the growth rate as

$$F_n=\frac{1}{E_n^2}\int_V \frac{R}{\overline{p}c_v}\psi_n\frac{\partial q'}{\partial t}dV \tag{9}$$

It can therefore be seen that modifying the distribution of heat release while not altering the aggregate value of $\overline{Q}$ is paramount when conducting a study intended to inspect the effects of burner configuration on growth rate.

The GIM heat release model was then modified to allow for the location, heat release area and distribution, and relative heat release density to be specified on a per element basis. This allowed for multiple configurations of burner assemblies to be analyzed to inspect the effect of geometric alterations on the growth rate of transverse mode shapes.

Scope of Study

The new model was then applied to a study to inspect the effect of asymmetrically staged elements on the growth rate of transverse modes. This section will describe the scope of the study.

It should be noted that when the term "fuel staging" is used in this study, it is referring to a relative fuel staging, described as

$$Fuel\ Staging_{relative}=\frac{\frac{\dot{m}_{B_{fuel}}}{\dot{m}_{A_{fuel}}}}{\frac{N_{B_{jets}}}{N_{A_{jets}}}}$$

For this study, the growth rate of a 1T transverse mode for three different configurations of staging for a generic burner were evaluated. The 1T transverse mode had a fixed orientation such that the pressure antinodes resided at 0° and 180°, or the left-most and right-most edges, as shown as Figure 2 [7].

The first configuration which was analyzed consisted of eight equally spaced elements. Figure 3 portrays the heat release profile of this first configuration. The next configuration to be tested, referred to as Configuration A, consisted of the same geometric alignment of the burners but with the two right-most and two left-most elements with a $Fuel\ Staging_{relative}$ = 2. The top-most and bottom-most elements remained with a $Fuel\ Staging_{relative}=1$. The last configuration analyzed, referred to as Configuration B, once again was comprised of the same

geometric alignment of the elements. However, for this condition the top-most and bottom-most elements were assigned a $Fuel\ Staging_{relative}$ = 2, while the two right-most and left-most elements had a $Fuel\ Staging_{relative}$ = 1.

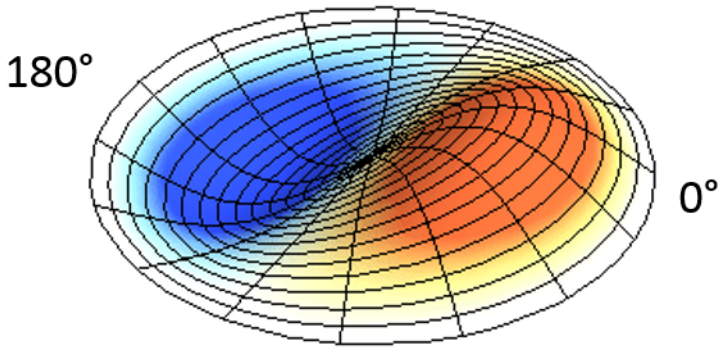

Figure 2. 1T mode shape example [7].

This heat release profile was then coupled with a 1T transverse mode and the corresponding growth rate was calculated. The resulting normalized Rayleigh index plots from these heat release profiles and 1T transverse mode shape are shown as Fig. 4. From the Rayleigh index plot, it can be seen that the burners residing in the location of the antinodes of the 1T mode shape are the largest contributors to the growth of the instabilities. This is represented by the dark red regions on the plot. Here it can be seen qualitatively that when the fuel staging was altered such that the densest regions of heat release were aligned with the antinodes of the transverse mode in Configuration A that the contributions of burners residing along the nodal line are minimal. Conversely, when the heat release was greatest at the elements which were aligned along the nodal line in Configuration B, those elements are qualitatively shown to have a higher contribution to the growth rate of the instability than the other test cases. However, because these Rayleigh index plots are normalized, Configuration B represents a more distributed growth profile and not a higher aggregate growth rate.

The growth rates of the 1T transverse modes coupled with the corresponding heat release profiles discussed is presented as Table 1. Here it can be seen that the Uniform Configuration had a 1T growth rate of 4.87, Configuration A had the highest calculated growth rate of 6.02, and Configuration B had the lowest calculated growth rate of 3.73. Therefore, it can be deduced that when the highest density of heat release along the 2D profile align with the antinodes of the transverse modes that the growth rate of the subsequent instability will be maximized. Likewise, the growth rate is minimized with the densest regions of heat release are located along the nodal line of the transverse modes.

1T Growth Rates	
Uniform Configuration	4.87
Configuration A	6.02
Configuration B	3.73

Table 1. Calculated growth rates of varied configurations.

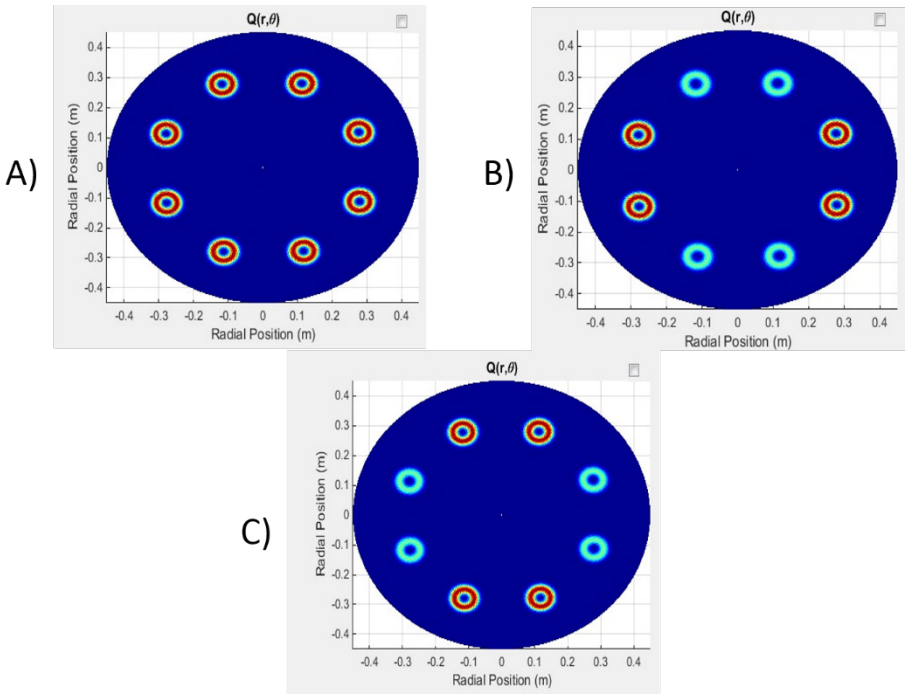

Figure 3. Heat release profiles for A) uniform burner configuration, B) Configuration A, and C) Configuration B.

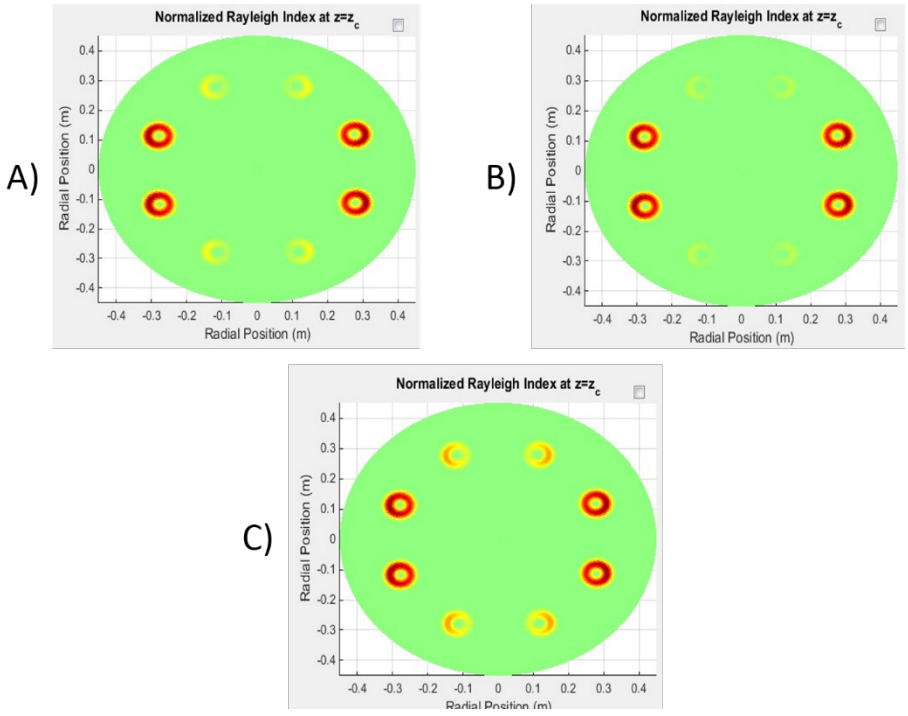

Figure 4. Normalized Rayleigh indices for A) uniform burner configuration, B) Configuration A, and C) Configuration B.

Conclusions

This study resulted in the following conclusions:

- Modifications were made to the mean heat release model to allow for per element modifications such as the specific positioning, relative fuel staging, and flame front location.
- The accuracy of growth rate prediction was increased due to these modifications.
- The calculated growth rate was maximized when the densest regions of heat release in the symmetric configurations aligned with pressure antinodes.

It can therefore be concluded that aligning the burners of the engine at the antinodes of a transverse mode results in higher growth rate of instabilities. However, it should be noted that these studies were performed corresponding to a fixed 1T mode shape orientation, and that in real applications the mode shape may shift corresponding to the characteristics of the system in which it develops.

Acknowledgements

Special thanks to the University Turbine Systems Research program of the Southwest Research Institute and to Siemens Energy.

References

[1] Coker A., Neumeier Y., Lieuwen T., Zinn B.T., Menon S., 2003, "Studies of Active Instability Control Effectiveness in a High Pressure, Liquid Fueled Combustor," AIAA Paper 2003-1009.

[2]Richards G.A., Straub D.L., Robey E.H., 2003, "Passive control of combustion dynamics in stationary gas turbines", AIAA Journal of Propulsion and Power, 19, 795-810.

[3] J.M. Pent, B.F. Kock, W. Krebs, and J.E. Portillo, "Application of a Generalized Instability Model to Industrial Annular Combustion Chambers", AIAA Paper 2012-0010, 50th AIAA Aerospace Sciences Meeting, Nashville, TN, January 09-12, 2012.

[4] Culick, F., "Unsteady Motions in Combustion Chambers for Propulsion Systems", *RTO AGARDograph,* AGAVT-039, 2006.

[5] Portillo, E. J., Sisco, J. C., Yu, Y., Anderson, W. E., "Application of a Generalized Instability Model to a Longitudinal Mode Combustion Instability", AIAA Paper 2007-XXXX, 43rd AIAA/ASME/SAE/ASEE Joint Propulsion Conference and Exhibit, Cincinnati, OH, July 8-11, 2007.

[6] Harrje, D., Reardon, F., "Liquid Propellant Rocket Combustion Instability, NASA SP194," NASA, Washington, D.C., 1972.

[7] Russel D.A., 1998 "Vibrational Modes of a Circular Membrane", Acoustics and Vibration Animations, The Pennsylvania State University, January 21, 1998.